Analytical model for two-channel phonon transport engineering

Tim Bernges*[a], Martin Peterlechner[b], Gerhard Wilde[b], Matthias T. Agne[a], Wolfgang G. Zeier*[a,c,d]

[a]*Institute of Inorganic and Analytical Chemistry, University of Münster, D-48149 Münster, Germany*

[b]*Institute of Materials Physics, University of Münster, D-48149 Münster, Germany*

[c]*International Graduate School for Battery Chemistry, Characterization, Analysis, Recycling and Application (BACCARA), University of Münster, D-48149 Münster, Germany*

[d]*Institut für Energie- und Klimaforschung (IEK), IEK-12: Helmholtz-Institut Münster, Forschungszentrum Jülich, 48149 Münster, Germany*

Corresponding author emails: tbernges@uni-muenster.de, wzeier@uni-muenster.de

Corresponding authors postal address: Corrensstraße 28/30, 48149 Münster

Abstract

The reduction of vibrational contributions to thermal transport and the search for material classes with intrinsically low lattice thermal conductivities are at the heart of thermoelectric research. Both engineering the heat transport of known thermoelectrics and searching for new material candidates is guided by understanding the physics of low thermal conduction. Spectral analytical models (e.g., the Callaway model) for propagating phonon transport have proved to be a powerful tool for interpreting experimental results and providing metrics for materials design. Now, however, it is known that another mechanism of phonon heat transport can occur in complex crystalline materials. Called diffusons, they describe the non-propagating atomic scale random-walk of thermal energy between energetically proximal phonon modes. While analytical models exist to describe both transport behaviors independently, an analytical model accounting for both transport channels simultaneously is necessary to interpret and design so-called 2-channel thermal transport. In this work, we propose an analytical 2-channel transport model that partitions the vibrational density of states into two transport regimes and subsequently accounts for both transport mechanisms. The model is then used to explain the experimental thermal conductivities of the solid solution series $Ag_{9-x}Ga_{1-x}Ge_xSe_6$. In this series, substitution leads to the stabilization of a highly vacant Ag^+ substructure, which is expected to induce strong point-defect phonon scattering. While the propagating phonons are strongly scattered at low temperatures, the diffuson channel is apparently unaffected. By establishing materials design metrics for 2-channel thermal transport from analytical theory, experimental investigations of materials with astonishingly low lattice thermal conductivities can now be better guided and informed.

Keywords: thermal transport, diffusons, argyrodites, two-channel transport, point defects, phonon engineering

1. Introduction

Engineering the lattice thermal conductivity of a material has significant importance for thermoelectrics,[1–3] thermal barrier coatings[4,5] and, as recently suggested, potential thermal management of solid-state batteries.[6–9] For example, lowering the lattice thermal conductivity directly improves the materials thermoelectric conversion efficiency.[1,10–12] Consequently, extensive efforts have been made in the thermoelectrics community to find and engineer materials with ultra-low thermal conductivities.[1,13] Originating from these efforts, a multitude of materials have been reported that show thermal transport behavior that cannot be explained by the classical description of heat transport by propagating phonons.[6,14,15] Propagating phonons, as described by the phonon-gas model (e.g., the Callaway model), propagate according to their group velocity in a particle-like manner analogous to a gas.[1,16,17] Propagating phonon transport considerations run into limitations once the magnitude of thermal conduction gets so low that the scattering rates associated with the propagating modes correspond to phonon mean-free-paths on the order of interatomic distances,[18,19] causing the phonon wavevector to be no longer well-defined (the so-called Ioffe-Regel limit).[20,21]

Materials reported to have ultra-low thermal conduction that cannot be explained only by this type of transport span a great variety of structures and compositions, e.g., $Yb_{14}(Mn,Mg)Sb_{11}$,[22] $La_2Zr_2O_7$,[21] $CsPbBr_3$,[17] $BaAg_2Te_2$[23] and LiS_2.[24] Another material class showing similar thermal transport behavior are the argyrodites,[25] where a multitude of compositions have been investigated for their use as thermoelectric materials, e.g., Ag_8GeSe_6,[26,27] Ag_9GaSe_6,[28,29] Ag_8SnSe_6[30,31] and Cu_7PSe_6.[32]

In these materials, especially at high temperatures, a fundamentally different description of thermal transport by phonons becomes necessary. Recently, we have suggested that the thermal transport of Ag_8GeSe_6 can be explained by the co-existance of propagating phonon modes

(phonon-gas model, propagons) and diffusons, a second type of phonon which does not propagate throughout the material and conducts heat diffusively.[27]

This second phonon channel of thermal transport, i.e., by diffusons,[20] fundamentally describes the thermal energy exchange between energetically proximal phonon modes resembling an atomic scale random walk between oscillators.[14,17,20] The exchange of vibrational energy is facilitated by a combination of small interband spacings (i.e., the energy difference between two phonon modes) and/or strong linewidth broadening (through anharmonicity especially at elevated temperatures) resulting in a high degree of quasi-degeneracy.[17,21] Consequently, significant diffuson contributions are found in materials with a large number of phonon modes in close energetic proximity (due to large complex unit cells, e.g., $Yb_{14}(Mg,Mn)Sb_{11}$[22]) or with strong linewidth broadening (e.g., $CsPbBr_3$[17]).

Often, even in ultra-low thermal conductivity materials, contributions from propagating phonon modes persist,[34,35] such that a model accounting for both transport processes becomes necessary. A theory accounting for both propagon (phonon-gas like) and diffuson transport in lattice dynamics calculations was recently developed by Simoncelli and coworkers[17,21] (and later extended by Hanus and coworkers[22]), and has since been applied to various materials,[34–36] including the Ag^+ argyrodite Ag_8GeSe_6.[27]

Given its strength in describing unintuitive thermal transport behavior, this expanded viewpoint of phonon character has sparked new interest in the thermal transport community.[14,17,22,27,37] Currently, the established 2-channel model[37] relies on lattice dynamical calculations, i.e., the phonon band structure as well as third (and higher) order force constants,[36] or molecular dynamics to distinguish propagons and diffusons[38,39] and to calculate the thermal transport contributions of both channels.[17,22,37] This makes assessing potential 2-channel transport in a material computationally expensive, especially for complex structures in which such transport is expected. Nevertheless, it was shown that an analytical

approximation for the phonon lifetimes can be used to reduce the computational cost of 2-channel modeling.[17,22] For computational and theoretical details of the 2-channel model, the reader is referred to the works by Simoncelli et al.,[17,21] Isaeva et al.,[35] Xia et al,[36] and Hanus et al.[22,37]

Expanding on the analytical approximations introduced to the 2-channel model,[22] we propose a fully analytical, spectral 2-channel model combining the established models for propagating transport, i.e., the Callaway-model,[1,37] and diffuson transport (the random-walk diffusion model[14]), in a straightforward fashion. At the core of this new model is the partition of the density of states into propagon and diffuson transport regimes. The proposed analytical 2-channel model is then utilized to investigate the thermal transport of the compositional series $Ag_{9-x}Ga_{1-x}Ge_xSe_6$, which reveals tremendous differences in its low temperature thermal conductivity behavior throughout the various substitution steps. Our analysis shows that Ag_9GaSe_6 conducts heat in a similar fashion to Ag_8GeSe_6,[27] with large propagon contributions at the lowest temperatures before transitioning to diffuson-dominated transport at elevated temperatures.[27] In contradistinction, the solid solutions $Ag_{9-x}Ga_{1-x}Ge_xSe_6$ show almost pure diffuson transport throughout the whole temperature range. This can be attributed to increased point-defect scattering of propagons, facilitated by the stabilization of the high-temperature argyrodite phase, consisting of a highly vacant Ag^+ substructure, to low temperatures.

This work shows that a spectral thermal transport model is applicable and valuable even in the presence of strong diffuson contributions and 2-channel transport, where new material design metrics are needed. By introducing an analytical model to describe experimentally determined lattice thermal conductivities, we aim to make considerations of 2-channel transport readily

accessible to experimentalists, thereby supporting the understanding of ultra-low thermal conductivities in complex crystalline solids.

2. Polymorphs of $Ag_{9-x}Ga_{1-x}Ge_xSe_6$ and phase analysis

Assessing and understanding the structure of a material is the first step in understanding all of its transport properties, including thermal transport.[1,16] The unit cell size,[1] the atomic species contained within the unit cell,[1,12] local structural features and mixed or partial occupations[40,41] have been shown to have tremendous effects on the transport of heat throughout the material.[17,37] The investigated compositions $Ag_{9-x}Ga_{1-x}Ge_xSe_6$, analogous to other common argyrodites like Li_6PS_5Cl[42] or Ag_8SnSe_6,[27,31] crystallize in the cubic space group $F\bar{4}3m$ at elevated temperatures. The crystal structure is built up from a rigid unit of $MSe_4^{(5-x)-}$ (M = Ge^{4+}, Ga^{3+}) tetrahedra and the characteristic, partially occupied (~23% fractional occupation) Ag^+ substructure.[27,43,44] The partially vacant substructure is often associated with the large ionic conductivities of the Ag^+ argyrodites and their Li^+ analogs,[25,42] providing sufficient vacant lattice sites for the mobile ion to jump. For simplicity, we will now refer to the $F\bar{4}3m$ phase as the cubic disordered phase, in reference to the structurally disordered Ag^+ substructure.

Below 283 K, Ag_9GaSe_6 crystallizes in the cubic space group $P2_13$,[45,46] which contrary to the high temperature phase is composed of a fully occupied Ag^+ substructure, in which Ag^+ cations are now located on clearly defined crystallographic sites. A similar transition to a phase with well-defined, fully occupied Ag^+ atomic positions occurs in Ag_8GeSe_6, which crystallizes in the orthorhombic phase $Pmn2_1$ below 323 K.[26,27] Visual representations of the unit cells of all phases are shown in the Supporting Information. In contrast to Ag_9GaSe_6 and Ag_8GeSe_6, thus far, there are no reports of phase transitions, i.e., an ordering of the Ag^+ substructure, in the solid solutions $Ag_{9-x}Ga_{1-x}Ge_xSe_6$ (x = 0.25, 0.50 and 0.75).

To gain information about the success of the synthesis and the stable polymorphs at intermediate and low temperatures, X-ray diffraction experiments were conducted at 298 K and 100 K, respectively. All Ga^{3+} containing compositions, e.g., $Ag_{9-x}Ga_{1-x}Ge_xSe_6$ (with x = 0.00, 0.25, 0.50 and 0.75), crystallize in the cubic disordered phase (space group $F\bar{4}3m$) at room temperature, as exemplary shown by Pawley fits of Ag_9GaSe_6 and $Ag_{8.5}Ga_{0.5}Ge_{0.5}Se_6$ (Figure 1 a, top panel). As mentioned beforehand, Ag_8GeSe_6 crystallizes in the orthorhombic phase $Pmn2_1$ below 323 K. At low temperatures (i.e., at 100 K), Ag_9GaSe_6 crystallizes in space group $P2_13$ in agreement with earlier reports (Figure 1 a, bottom panel).[29,46] Contrary, the solid solutions $Ag_{9-x}Ga_{1-x}Ge_xSe_6$ (x = 0.25, 0.50 and 0.75) exist in the cubic disordered phase even at 100 K (exemplarily shown for x = 0.5, Figure 1 a, bottom panel). All diffractograms and corresponding Pawley fits are shown in the Supporting Information (Figure S2, Table S1). The successful formation of the solid solution is verified by the decrease of the unit cell volume (normalized to the number of formula units per unit cell Z) with the substitutional degree (Figure 1 b), caused by both, the decreasing amount of Ag^+ contained within the cell upon replacing Ga^{3+} with Ge^{4+}, and the lower ionic radius of Ge^{4+} (0.39 Å)[47] compared to Ga^{3+} (0.47 Å).[47]

In conclusion, the structural analyses reveal that the complex, partially occupied Ag^+ substructure is chemically stabilized in $Ag_{9-x}Ga_{1-x}Ge_xSe_6$ (x = 0.25, 0.50 and 0.75), as compared to the structural ordering of Ag^+ that occurs in Ag_9GaSe_6 and Ag_8GeSe_6 at lower temperatures.[25,27,29] Later it is shown that the difference in the Ag^+ substructure, being either fully occupied (structurally ordered) or partially occupied (structurally disordered), causes tremendous differences in the thermal transport behavior at low temperatures (<100 K).

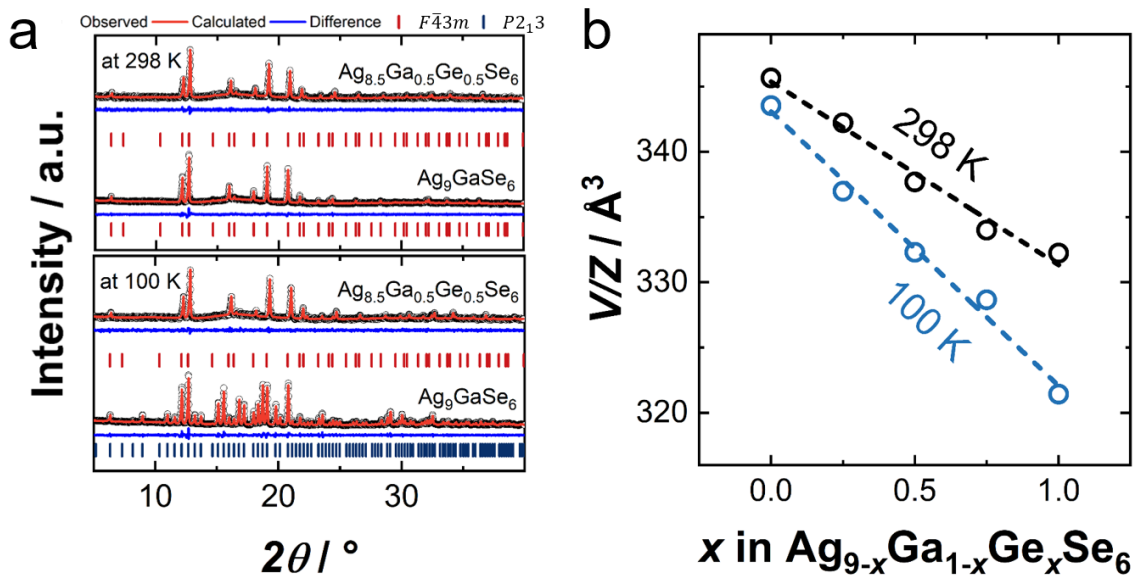

Figure 1. a) Pawley fits against X-ray diffraction data. top) At room temperature, both, Ag_9GaSe_6 and the solid solutions (exemplarily shown: $Ag_{8.5}Ga_{0.5}Ge_{0.5}Se_6$) crystallize in the cubic disordered phase (space group $F\bar{4}3m$). bottom) At 100 K, the solid solutions still crystallize in the cubic disordered phase, while Ag_9GaSe_6 undergoes Ag^+ structural ordering and crystallizes in the cubic ordered phase $P2_13$. b) Unit cell volume as a function of the substitutional degree (normalized to the number of formula units per unit cell Z), showing the successful formation of the solid solutions.

3. Thermal transport of $Ag_{9-x}Ga_{1-x}Ge_xSe_6$

The thermal conductivities of the series $Ag_{9-x}Ga_{1-x}Ge_xSe_6$ were experimentally determined in a temperature range from 2 K to 600 K, with the goal to investigate the influence of the discussed changes to the Ag^+ substructure, i.e., being either fully occupied and structurally ordered or partially vacant and structurally disordered. As we reported and discussed the thermal transport of Ag_8GeSe_6 in an earlier work,[27] here these results are shown again to complement the results of the solid solution series.[27] Most investigated samples showed negligible electronic contributions to the thermal conduction κ_e, such that the measured total thermal conductivity $\kappa = \kappa_e + \kappa_L$ can be considered equal to only the lattice thermal conductivity, i.e., $\kappa \approx \kappa_L$,

contributed by phonon heat transport. The electronic transport data and the electronic contributions to the thermal conductivity of all materials are shown in the Supporting Information (Figure S4 to S7).

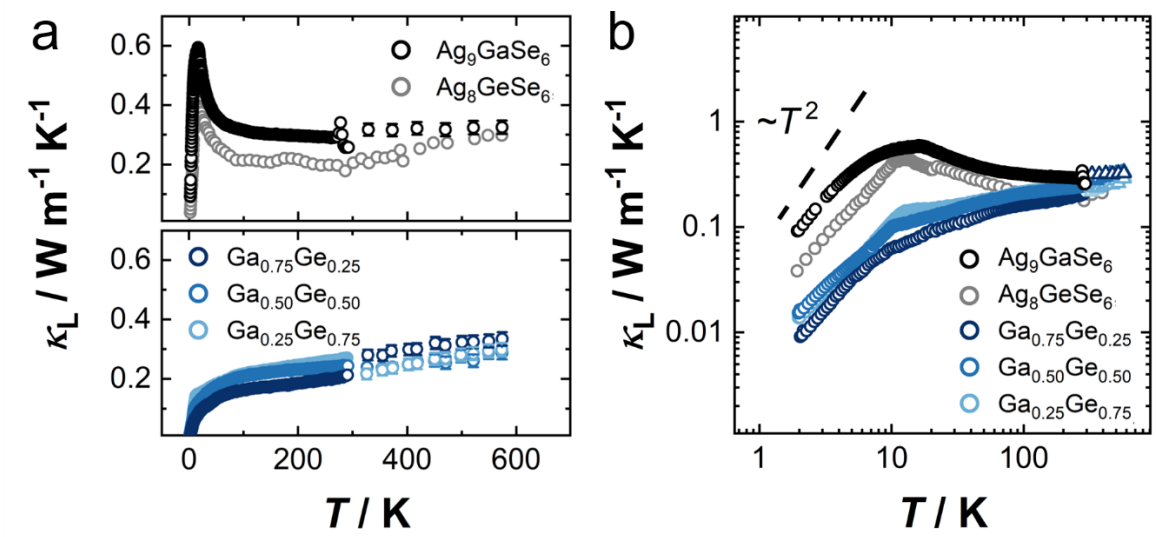

Figure 2. *a) Lattice thermal conductivity of $Ag_{9-x}Ga_{1-x}Ge_xSe_6$. top) Both endmembers, i.e., Ag_9GaSe_6 and Ag_8GeSe_6,*[27] *show a phonon peak in thermal conduction at low temperatures which leads into almost constant behavior at higher temperatures (>100 K). bottom) The solid solutions $Ag_{9-x}Ga_{1-x}Ge_xSe_6$ (x = 0.25, 0.50 and 0.75) show no clearly pronounced phonon peak, but instead a steady increase of the thermal conductivity upon heating. b) A logarithmic plot of the results in panel a showing $\kappa_L \propto T^2$ at the lowest temperatures, which is expected when propagating phonons are predominantly scattered by dislocations (e.g. at grain boundaries).*

The lattice thermal conductivities of the solid solutions $Ag_{9-x}Ga_{1-x}Ge_xSe_6$ show significant differences in their temperature dependencies at low temperatures (<100 K), comparing Ag_9GaSe_6 and Ag_8GeSe_6[27] (Figure 2 a, top) to the compositions with mixed Ga^{3+} and Ge^{4+} site occupation (Figure 2 a, bottom). The thermal conductivity of Ag_9GaSe_6 is comparable to the thermal conductivity of Ag_8GeSe_6,[27] characterized by $\kappa_L \propto T^2$ at the lowest temperatures that is consistent with scattering of propagating phonons by dislocations (e.g. at grain boundaries),[2] followed by a so-called phonon peak at ~12 K and then an approximately

constant value of $\kappa_L \approx 0.31$ W m^{-1} K^{-1} at elevated temperatures (>100 K, Figure 2 a). It should be noted that a peak in thermal conductivity is expected from classic phonon-gas theory when the dominant scattering mechanism transitions from microstructural scattering at low temperature to phonon-phonon scattering at high temperature, and so a "phonon peak" is indicative of phonon-gas transport. [1,3,16] Although a phonon peak is observed in Ag_8GeSe_6, it was shown previously that the full temperature dependence of κ_L requires 2-channel transport considerations, with significant contributions by both, propagons and diffusons.[27] Considering 2-channel transport, the $\kappa_L \propto T^2$ behavior and the phonon peak can be explained by dominating propagon (phonon-gas like) transport at low temperatures, while the approximately constant thermal conductivities at intermediate and high temperatures are in agreement with diffuson transport considerations.[22,27] Thus, from a visual comparison of the thermal conductivities of Ag_9GaSe_6 and Ag_8GeSe_6 (Figure 2 top),[27] similar transport physics, i.e., 2-channel thermal transport, are expected in Ag_9GaSe_6.

Contrary to the endmembers, no clearly pronounced phonon peak can be observed in the solid solutions $Ag_{9-x}Ga_{1-x}Ge_xSe_6$ (x = 0.25, 0.50 and 0.75, Figure 2 bottom), but a continuous increase of the thermal conductivity upon heating. At the lowest temperatures, the thermal conductivities increase approximately as $\kappa_L \propto T^2$, similar to the results of Ag_9GaSe_6 and Ag_8GeSe_6.[27] A log-log plot of the thermal conductivities emphasizes the low temperature proportionality of all compositions (Figure 2 b). Again, this is in line with the expected temperature dependence originating from the scattering of propagating phonons by the materials microstructure (often called boundary scattering) and indicates the presence of propagon contributions to thermal transport[2,37] despite the absence of a clearly pronounced phonon peak. At the same time, the almost temperature independent, slightly increasing thermal conductivities from 100 K to 600 K (Figure 2 bottom) strongly suggest significant diffuson contributions.[20,48,49]

These observations suggest that 2-channel transport, as recently shown in Ag_8GeSe_6,[27] is also likely in Ag_9GaSe_6 and the solid solutions $Ag_{9-x}Ga_{1-x}Ge_xSe_6$ (x = 0.25, 0.50 and 0.75). Given the significant differences in the temperature dependence of thermal conductivity at low temperatures (<100 K) there is the outstanding question of how point-defects (i.e., the disordered Ag^+ substructure) may influence both the propagon and diffuson type transport. Herein, an analytical 2-channel model is developed to answer these questions, in which the model parameters give crucial insights to the nature of phonon transport across the full temperature range. In particular, the conducted 2-channel analysis reveals that point-defects originating from the partially occupied Ag^+ substructure, have a large impact on propagons (i.e., suppressing the phonon peak at low temperatures), but seem to have negligible influence on diffusons.

4. Analytical 2-channel model

Analytical modeling of thermal transport has significant importance for experimental studies, as it allows investigating the microscopic origin of macroscopically determined thermal conductivities.[1] Historically, the majority of analytical thermal transport modeling has relied on a spectral description of phonons, like the Callaway model,[1,50] in which all phonons are treated as propagating and phonon-gas like (propagons).[37] Thus, the Callaway model has been used to investigate changes to the phonon (group) velocities, e.g., through lattice softening[3,51] and avoided-crossings,[13,52] and changes to the phonon scattering rates, e.g., through boundary,[2] phonon-phonon and point-defect scattering,[40] in crystalline materials. It has been previously recognized that the Callaway model tends to overestimate the thermal conductivity of complex crystals, with various modifications introduced to account for non-dispersive optical phonons.[1,19,53] At the same time, a thermal transport model for amorphous materials was developed, which classifies phonons into three types, i.e., propagons, diffusons and locons,[20] and associates each phonon type with a frequency range in the vibrational

spectrum. Empirically, the low frequency (acoustic) vibrations are propagons and higher frequency (optical) vibrations tend to have diffuson character (see schematic in Figure 3).[17]

Based on the current understanding of 2-channel transport in both crystalline and amorphous materials, the total lattice thermal conductivity κ_{L} can thus be written as:[17,22]

$$\kappa_{\mathrm{L}} = \kappa_{\mathrm{pr}} + \kappa_{\mathrm{diff}}, \qquad \text{Eq. 1}$$

where κ_{pr} and κ_{diff} denote the contributions of propagons (phonon-gas like transport) and diffusons to the thermal conductivity. Given the recent interest to characterize 2-channel transport, but recognizing the computational limitations associated with complex defective materials, an analytical spectral model, building upon the Callaway model but accounting for the possibility of diffuson contributions, is a timely and much-needed tool.

Herein, in agreement with earlier work by Snyder et al.,[54] we propose to divide the phonon density of states into two transport regimes, and use the Callaway model[1] to describe the thermal transport by propagons and the random-walk diffusion model[14] for diffusons (short overview and visual summary in Figure 3). The influence of any localized modes (locons) is implicitly captured by the average diffuson diffusivity characterized by *P* within the random-walk diffusion model,[14] as discussed later.

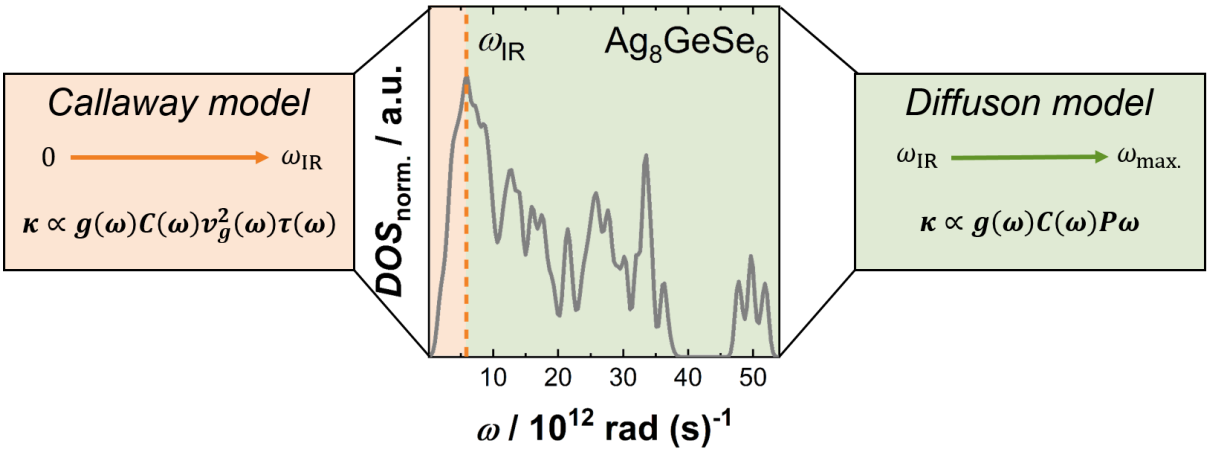

Figure 3. *Schematic visualization of the proposed analytical 2-channel model. left) The Callaway model is utilized to describe thermal transport contributions by all phonon modes below the transition frequency* ω_{IR}*, which behave in a gas-like manner. middle) A transition frequency is introduced to differentiate the propagon (orange shading) and diffuson (green shading) regimes. right) Above the transition frequency, phonon modes are treated as conducting thermal energy diffuson-like (green shading). The diffuson contributions are described by the random-walk diffusion model introduced by Agne et al.*[14]

4.1. The propagon and diffuson regimes

Frequently, analytical thermal conductivity models are based on the Debye approximation, which assumes constant group velocities throughout the entire Brillouin zone.[16] This approximation is often inaccurate for complex materials given the large number of nearly dispersionless optical phonon branches. For these complex cases, Chen et al.[53] and Toberer et al.[1] developed analytical models that distinguish the thermal transport contributions originating from acoustic and optical modes, using a maximum phonon scattering model for optical phonons.[54] A similar methodology is utilized in this work, with important distinctions. First, we incorporate a physical model of diffuson transport, which is defined by fundamentally different metrics than phonon scattering models. Second, we utilize the phonon density of states

(e.g., calculated from density functional theory or determined from inelastic neutron- or X-ray scattering experiments) directly, without making the Debye model approximation. Using a better estimation of the phonon density of states is important for capturing the temperature dependence and magnitude of diffuson contributions to the thermal conductivity. Given the widespread availability of lattice dynamics calculations and the well-known limitations of the Debye model, this is a valuable update to analytical thermal transport modeling.

Following previous observations that acoustic modes conduct heat as propagons while optical modes are expected to conduct heat diffuson-like,[17,21,27,38] we partition the density of states at the acoustic phonon cut-off frequency (Figure 3). Using the terminology introduced by Allen and coworkers we call this the Ioffe-Regel frequency ω_{IR}, and estimate it as $\omega_{\mathrm{IR}} = \omega_{\mathrm{D}} N^{-1/3}$ defined by the Debye frequency $\omega_{\mathrm{D}} = (6\pi^2 n)^{1/3} v_{\mathrm{s}}$ (using the number density of atoms n in units of atoms m^{-3} and the mean speed of sound v_{s}) and the number of atoms per primitive unit cell N, as previously suggested by Toberer and coworkers.[1] While the transition frequency between propagons and diffusons can be determined more accurately using molecular dynamics calculations,[38] our first-order estimate is expected to be sufficient to capture the essential physics of 2-channel thermal transport.

Having assigned the respective frequency ranges for propagons and diffusons, the analytical models that describe the thermal transport of the different phonon types can be applied.[1,14,37] The Callaway model[1,3,50] describes the thermal transport of propagating modes and can thus be used for the thermal conductivity of the propagon-channel κ_{pr}:

$$\kappa_{\mathrm{pr}} = \frac{3nk_{\mathrm{B}}}{3} \int_0^{\omega_{\mathrm{IR}}} \frac{g(\omega)}{3n} C(\omega) v_{\mathrm{g}}^2(\omega) \tau(\omega) \mathrm{d}\omega. \qquad \text{Eq. 2}$$

In the Callaway model, phonon modes transport heat according to their spectral heat capacity $C(\omega)$, group velocity $v_{\mathrm{g}}(\omega)$ and relaxation time $\tau(\omega)$, where the latter depends on the scattering processes at play in the material.[2,16,37,40] The number density of atoms n is utilized in the

normalization of the phonon density of states $g(\omega)$ (with $\int_0^\infty \left(\frac{g(\omega)}{3n}\right) \mathrm{d}\omega = 1$). The spectral heat capacity $C(\omega)$ is defined from Bose-Einstein statistics as:[14]

$$C(\omega) = \left(\frac{\hbar\omega}{k_\mathrm{B}T}\right)^2 \left(e^{\frac{\hbar\omega}{k_\mathrm{B}T}}\right)\left(e^{\frac{\hbar\omega}{k_\mathrm{B}T}} - 1\right)^{-2}. \quad \text{Eq. 3}$$

Above the Ioffe-Regel crossover frequency $\omega > \omega_\mathrm{IR}$, phonon modes are treated as diffusons and their thermal conductivity κ_diff can be calculated according to the random-walk diffusion model introduced by Agne et al.:[14,37]

$$\kappa_\mathrm{diff} = \frac{n^{\frac{1}{3}} k_\mathrm{B}}{\pi} \int_{\omega_\mathrm{IR}}^{\infty} \frac{g(\omega)}{3n} C(\omega) P\, \omega \, \mathrm{d}\omega. \quad \text{Eq. 4}$$

Here, P defines an average thermal energy exchange rate between diffuson modes, a short discussion of which will follow later.[14] Substituting Eq. 2 and Eq. 4 in Eq. 1 leads to the expression of the lattice thermal conductivity:

$$\kappa_\mathrm{L} = \frac{3nk_\mathrm{B}}{3} \int_0^{\omega_\mathrm{IR}} \frac{g(\omega)}{3n} C(\omega) v_\mathrm{g}^2(\omega) \tau(\omega) \mathrm{d}\omega + \frac{n^{\frac{1}{3}} k_\mathrm{B}}{\pi} \int_{\omega_\mathrm{IR}}^{\infty} \frac{g(\omega)}{3n} C(\omega) P\, \omega \, \mathrm{d}\omega. \quad \text{Eq. 5}$$

4.2. Analytical modeling of the propagon channel

To determine κ_pr (Eq. 2), we use $g(\omega)$ directly (as determined by lattice dynamics calculations or from experiment) and use the average speed of sound v_s as an estimate for the phonon group velocity $v_\mathrm{g}(\omega) \approx v_\mathrm{s}$, which is a common approximation in describing the phonon transport of acoustic modes.[1]

Then, the total phonon lifetime $\tau(\omega)$ needs to be estimated. Multiple scattering sources are accounted for by summing the constituent phonon lifetimes according to Matthiessen's rule

(Eq. 5).[1] In agreement with typical Callaway modeling procedures, phonon-phonon scattering $\tau_{\mathrm{ph}}(\omega)$, boundary scattering $\tau_{\mathrm{gb}}(\omega)$ and point-defect scattering $\tau_{\mathrm{pd}}(\omega)$ are considered, leading to:

$$\tau^{-1}(\omega) = \tau_{\mathrm{ph}}^{-1}(\omega) + \tau_{\mathrm{gb}}^{-1}(\omega) + \tau_{\mathrm{pd}}^{-1}(\omega) \quad \text{Eq. 6}$$

$$= C_1\omega^2 T + A\omega + C_2\omega^4, \quad \text{Eq. 7}$$

as the full analytical description of the spectral phonon relaxation time $\tau^{-1}(\omega)$.[1,37,40] Generally, C_1, A and C_2 are the model parameters that can be fit to the experimental data. Estimating the magnitude of each parameter from a physical understanding is advised to validate the empirical results. A brief overview of how to estimate the magnitude of each parameter is given in the Supporting Information.

4.3. Analytical modeling of the diffuson channel

While the Callaway model requires an approximation of the phonon lifetimes,[1] in the diffuson model, it is *P* that is needed to describe the average diffuson diffusivity (Eq. 4).[14] In the derivation of the analytical diffuson model,[14] $P = 1$ conceptually describes a maximum rate of thermal energy transfer between diffuson modes.[14] In this work we use *P* as a fitting parameter to experimentally determine the average coupling between diffuson modes. Currently, there is limited understanding about the physics underlying *P*, although we expect it to be related to the degree of overlap (quasi-degeneracy) between phonon modes that enables diffuson transport. The case of $P = 1$ describes full degeneracy between all vibrational modes, while in reality, the overlap of the modes is dependent on both, their proximity in energy (frequency) and linewidth broadening (conceptually shown in Supporting Information). With that, we currently believe that *P* is related to the average overlap integral of each pair of vibrational modes and that *P* can be both, frequency and temperature dependent. To strengthen the physical understanding of *P*, a comparison of ab-initio 2-channel modeling results and

calculated overlap integrals (i.e., evaluating the degree of degeneracy) with the fitting results using the analytical 2-channel model are required in the future.

5. Application of the analytical 2-channel model

The analytical model proposed herein successfully describes the reported thermal conductivity of Ag_8GeSe_6[27] using the calculated vibrational density of states,[27] the measured speed of sound,[27] and fitting the phonon scattering parameters C_1, A and C_2, and the diffuson diffusivity parameter P (Figure 4). Specifically, the analytical model reproduces the magnitude and temperature dependence of the propagon and diffuson channel, and the total lattice thermal conductivity of the previously reported lattice dynamics based 2-channel modeling of Ag_8GeSe_6.[27] A direct comparison and a detailed description of the modeling procedure is included in the Supporting Information (Figure S8). The fitted parameters obtained from regression analysis are in reasonable vicinity to those determined from lattice dynamical calculations, especially considering the strong simplifications in the analytical model (Table S3, Supporting Information).

Given the apparent similarities in the temperature dependence of the thermal conductivity between Ag_8GeSe_6 and Ag_9GaSe_6 (Figure 2), the same modeling procedure was conducted for Ag_9GaSe_6, utilizing the measured sound velocity and the calculated vibrational density of states of Ag_8GeSe_6. All speeds of sound and modeling parameters are listed in Table S2 in the Supporting Information.

The decision to use the same vibrational density of states (i.e., Ag_8GeSe_6)[27] is motivated by the fact that changes to the chemical composition are minor and Ag^+ argyrodites, e.g., Ag_9GaSe_6,[29] and Ag_8SnSe_6,[31] are known to have similar vibrational properties. Thus, the density of states of Ag_8GeSe_6 is expected to be a good approximation for the series $Ag_{9-x}Ga_{1-x}Ge_xSe_6$. Recently, a high-throughput methodology has been proposed that is expected to provide similarly reasonable estimates of the vibrational density of states, and may

be particularly useful when considering large unit cells, and to access vibrational densities of states necessary for analytical 2-channel modeling of other material classes.[55] Although the distribution of vibrational states in the $Ag_{9-x}Ga_{1-x}Ge_xSe_6$ series is expected to be similar, it is still not known to what extend a large number of point-defects, as introduced by the stabilization of the Ag^+ structural disorder to low temperatures in the solid solutions, may impact phonon transport behavior in this known 2-channel system.

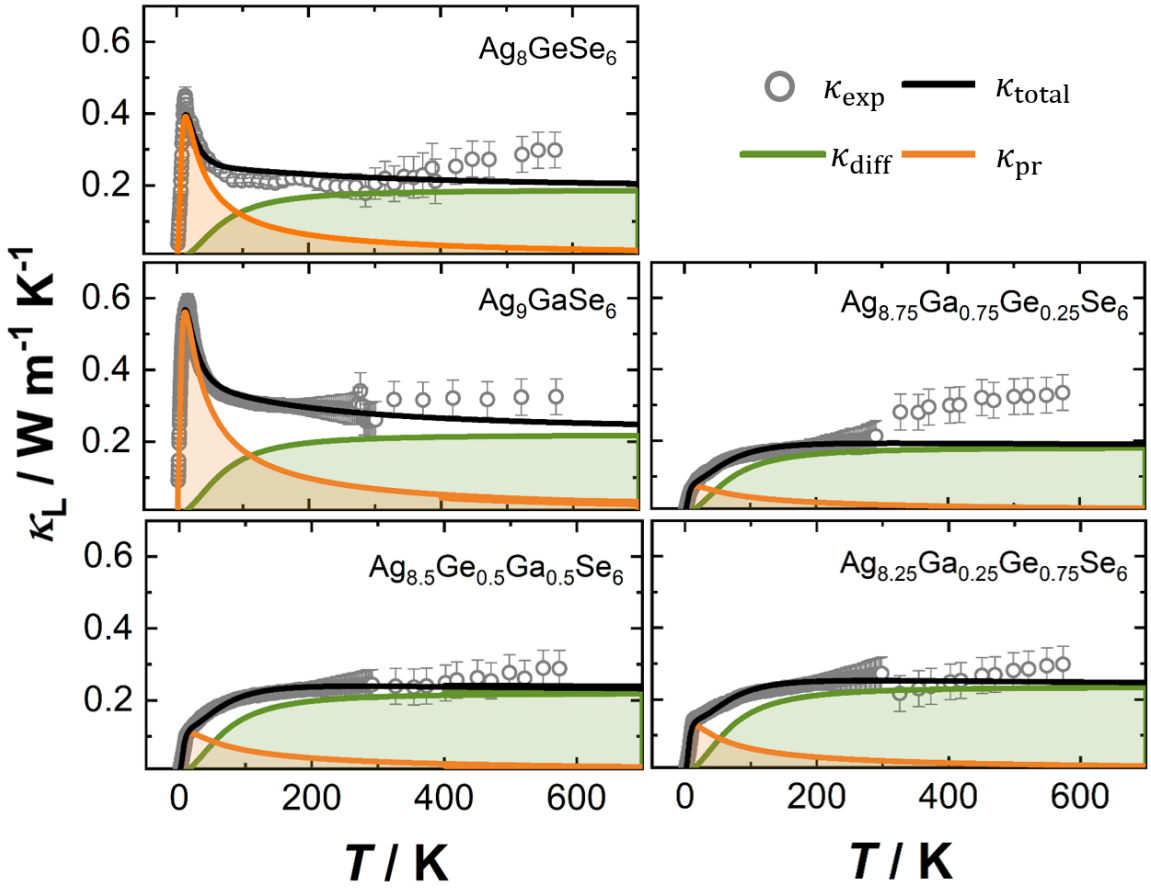

Figure 4. *Analytical 2-channel modeling of $Ag_{9-x}Ga_{1-x}Ge_xSe_6$. The analytical 2-channel model leads to a good description of the experimental results for all samples and successfully reproduces the reports about Ag_8GeSe_6.*[27] *The uncertainties of the LFA data (>300 K) are approximated by the expected experimental standard deviations based on the work by Lin et al.*[29] *Similar to Ag_8GeSe_6, Ag_9GaSe_6 shows significant propagon contributions to thermal conduction at low temperatures, leading to a pronounced phonon peak. Contrary, the absence*

of a clearly pronounced phonon peak in the solid solutions $Ag_{9-x}Ga_{1-x}Ge_xSe_6$ (x = 0.25, 0.50 and 0.75) can be explained by additional scattering of the propagating phonons by point-defects.

From chemical intuition, an influence of point-defect scattering on the propagon channel can be expected, as the Ag^+ substructure in the solid solutions is only ~23 % occupied and there is a large mass difference associated with an Ag^+ ion occupying a previously vacant site. While the substitution of Ga^{3+} with Ge^{4+} can introduce additional point-defect scattering, we expect the effect to be negligible given the lower mass contrast compared to the heavy Ag^+ defects. Following these considerations, the point-defect scattering term is expected to be significantly larger when the analytical model (Eq. 6 and Eq. 7) is fit to the experimental data of the solid solutions. This is indeed the case, and an accurate description of the thermal transport in all solid solutions is achieved by regression analysis with the analytical 2-channel model, again, over the entire temperature range (Figure 4). Given the larger deviation between the low and high temperature lattice thermal conductivities of $Ag_{8.75}Ga_{0.75}Ge_{0.25}Se_6$, the model was only fit against the low temperature results (to not negatively influence the low temperature fit results). All input and model parameters are listed in the Supporting Information (Table S3). From this analysis, it is shown that the significantly increased point-defect scattering substantially suppresses the phonon-peak, so that it becomes no longer clearly pronounced in the solid solutions as compared to Ag_8GeSe_6[27] and Ag_9GaSe_6 (Figure 2). Moreover, our analysis reveals a change of the boundary scattering term (i.e., A) comparing the solid solutions and the endmembers, which motivates further studies focused on the influence of point-defects on the microstructure in the argyrodites class as has been observed in PbSe.[56] Nevertheless, the observed $\kappa_L \propto T^2$ behavior at the lowest temperatures (<3 K) originating from scattering on dislocations (e.g., grain boundaries) is still accurately described.[2] It has to be noted that while a strong increase of point-defect scattering in the solid solutions is observed compared to the

endmembers, we were not able to resolve a compositional trend due to the generally low thermal conductivities and the associated measurement uncertainties. Similarly, although the value of P was found to vary somewhat between the different compositions, there is no strong indication at this time that point-defects significantly impacts the diffuson channel. Nonetheless, minimizing experimental uncertainty in thermal conductivity measurements will be necessary to distinguish the changes in P that may be possible by tuning the vibrational density of states.[22]

To visualize how each scattering coefficient (Eqs. 5 and 7) impacts κ_{L}, Figure 5 shows how the propagon contributions to the thermal conductivity change as the scattering parameters are varied from those determined for Ag_9GaSe_6 towards those determined for the solid solution $Ag_{8.5}Ga_{0.5}Ge_{0.5}Se_6$. This comparison emphasizes that the difference in magnitude and temperature dependence of thermal transport originates in a large part from the increased number of point-defects (and the corresponding change in C_2). Again, this is expected following the stabilization of the cubic disordered phase to low temperatures, leading to a large number of intrinsic (heavy) point-defects. Our analysis additionally suggests an influence of point-defects on the microstructure (i.e., A), the understanding of which requires further studies. Contrary, the smaller variations of the phonon-phonon scattering term (i.e., C_1) only have minor influences on the propagon channel (Figure 5). It should be noted that the relatively subtle changes observed in phonon-phonon scattering are likely within the range expected considering measurement uncertainties, however the necessity and predominance of point-defect scattering in the disordered materials is clear by the strong suppression of the phonon peak.

Thus, the introduction of the analytical model guided our understanding of the experimental results, especially at low temperatures, revealing significant impact of point-defects on propagon transport. This influence of point-defects cannot be directly assessed from the high temperature thermal conductivity of the argyrodites when diffusons dominate thermal transport,

and based on our current understanding, diffusons are independent of both static and dynamic point-defects in the argyrodites.[27] With that, it is shown that tracking scattering parameters and the diffuson diffusivity parameter using the analytical model has the potential of tracing the influence of structural and chemical changes on the lattice thermal conductivity in other 2-channel conducting materials in the future.

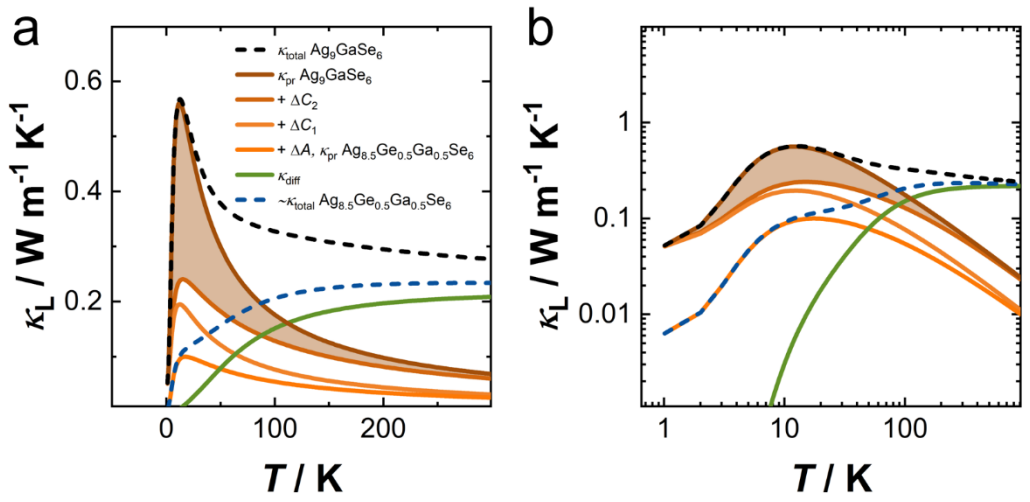

Figure 5. *a) Influence of the model parameters on the propagon channel. Starting from the modeling results of Ag_9GaSe_6, subsequently, variations of point-defect scattering (denoted: + ΔC_2), phonon-phonon (denoted: + ΔC_1) and boundary scattering (denoted: + ΔA) compared to $Ag_{8.5}Ga_{0.5}Ge_{0.5}Se_6$ are introduced. This visualizes the influence of each parameter on the model. It is shown that a large portion of the change in thermal transport at low temperatures (~10 K) can be explained by increased point-defect scattering. Variations of the diffuson channel are not shown for clarity. b) A logarithmic plot of panel a.*

6. Conclusion

In this work, 2-channel thermal transport, by both propagons and diffusons, was shown to be prevalent in all compositions within the solid solution series $Ag_{9-x}Ga_{1-x}Ge_xSe_6$. In Ag_9GaSe_6, in agreement with previous results on Ag_8GeSe_6, propagating phonon transport dominates at the lowest temperatures, as indicated by the typical temperature dependencies originating from

boundary and phonon-phonon scattering. Contrary, at intermediate and high temperatures, diffuson type conduction is responsible for the majority of heat transport, leading to the typical flat temperature dependence frequently reported for the argyrodites material class. In the intermediate compositions of the solid solutions, the highly vacant and disordered Ag^+ substructure associated with the argyrodites high temperature phase, is stabilized to low temperatures. In agreement with the strong structural disorder, point-defect scattering makes a significant impact on the propagon transport channel, leading to the suppression of the phonon peak and diffuson dominated transport throughout almost the entire temperature range, as determined by the proposed analytical 2-channel model. In first approximation, the magnitude of diffuson transport was found to be independent of the additional scattering of the propagon channel by point-defects. These results suggest that typical strategies of engineering thermal transport, based on the scattering of propagating phonons, will only influence the transport at low temperatures in complex crystalline materials dominated by diffuson transport at high temperature. Therefore, we suggest that design principles targeting diffuson transport directly need to be developed, which should include characterizing the distribution of the vibrational states (e.g., interband spacings), and the degree of their (quasi)degeneracy at elevated temperatures (e.g., linewidth broadening). We believe that the introduction of this analytical 2-channel transport model can facilitate 2-channel transport considerations and help establish engineering design principles of thermal transport in complex crystalline materials.

Acknowledgements

The research was supported by the Deutsche Forschungsgemeinschaft (DFG) under grant number ZE 1010/5-1. M.T.A. acknowledges the Alexander von Humboldt Foundation for financial support through a Postdoctoral Fellowship.

Data availability

Research data are available from the corresponding authors upon reasonable request.

Supplementary data

The experimental procedures, X-ray analyses, electronic transport characterizations and additional information about the modeling procedure can be found in the Supplementary data.

References

[1] E.S. Toberer, A. Zevalkink, G.J. Snyder, Phonon engineering through crystal chemistry, J. Mater. Chem. 21 (2011) 15843–15852. https://doi.org/10.1039/c1jm11754h.

[2] R. Hanus, A. Garg, G.J. Snyder, Phonon diffraction and dimensionality crossover in phonon-interface scattering, Commun. Phys. 1 (2018) 1–11. https://doi.org/10.1038/s42005-018-0070-z.

[3] R. Hanus, M.T. Agne, A.J.E. Rettie, Z. Chen, G. Tan, D.Y. Chung, M.G. Kanatzidis, Y. Pei, P.W. Voorhees, G.J. Snyder, Lattice Softening Significantly Reduces Thermal Conductivity and Leads to High Thermoelectric Efficiency, Adv. Mater. 21 (2019) 1900108. https://doi.org/10.1002/adma.201900108.

[4] D.R. Clarke, Materials selections guidelines for low thermal conductivity thermal barrier coatings, Surf. Coatings Technol. 163–164 (2003) 67–74. https://doi.org/10.1016/S0257-8972(02)00593-5.

[5] R. Vaßen, M.O. Jarligo, T. Steinke, D.E. Mack, D. Stöver, Overview on advanced thermal barrier coatings, Surf. Coatings Technol. 205 (2010) 938–942. https://doi.org/10.1016/j.surfcoat.2010.08.151.

[6] Z. Cheng, B. Zahiri, X. Ji, C. Chen, D. Chalise, P. V. Braun, D.G. Cahill, Good Solid-State Electrolytes Have Low, Glass-like Thermal Conductivity, Small 28 (2021)

2101693. https://doi.org/10.1002/smll.202101693.

[7] J. Shin, S. Kim, H. Park, H. Won Jang, D.G. Cahill, P. V. Braun, Thermal conductivity of intercalation, conversion, and alloying lithium-ion battery electrode materials as function of their state of charge, Curr. Opin. Solid State Mater. Sci. 26 (2022) 100980. https://doi.org/10.1016/j.cossms.2021.100980.

[8] T. Bernges, T. Böger, O. Maus, P.S. Till, M.T. Agne, W.G. Zeier, Scaling Relations for Ionic and Thermal Transport in the Na^+ Ionic Conductor Na_3PS_4, 4 (2022) 2491-2498. https://doi.org/10.1021/acsmaterialslett.2c00846.

[9] M.T. Agne, T. Böger, T. Bernges, W.G. Zeier, Importance of Thermal Transport for the Design of Solid-State Battery Materials, PRX Energy. 1 (2022) 031002. https://doi.org/10.1103/PRXEnergy.1.031002.

[10] G.J. Snyder, E.S. Toberer, Complex thermoelectric materials., Nat. Mater. 7 (2008) 105–114. https://doi.org/10.1038/nmat2090.

[11] A. Zevalkink, D.M. Smiadak, J.L. Blackburn, A.J. Ferguson, M.L. Chabinyc, O. Delaire, J. Wang, K. Kovnir, J. Martin, L.T. Schelhas, T.D. Sparks, S.D. Kang, M.T. Dylla, G.J. Snyder, B.R. Ortiz, E.S. Toberer, A practical field guide to thermoelectrics: Fundamentals, synthesis, and characterization, Appl. Phys. Rev. 5 (2018). https://doi.org/10.1063/1.5021094.

[12] W.G. Zeier, A. Zevalkink, Z.M. Gibbs, G. Hautier, M.G. Kanatzidis, G.J. Snyder, Thinking Like a Chemist: Intuition in Thermoelectric Materials, Angew. Chemie - Int. Ed. 55 (2016) 6826–6841. https://doi.org/10.1002/anie.201508381.

[13] M. Christensen, A.B. Abrahamsen, N.B. Christensen, F. Juranyi, N.H. Andersen, K. Lefmann, J. Andreasson, C.R.H. Bahl, B.B. Iversen, Avoided crossing of rattler modes in thermoelectric materials, Nat. Mater. 7 (2008) 811–815.

https://doi.org/10.1038/nmat2273.

[14] M.T. Agne, R. Hanus, G.J. Snyder, Minimum thermal conductivity in the context of: Diffuson -mediated thermal transport, Energy Environ. Sci. 11 (2018) 609–616. https://doi.org/10.1039/c7ee03256k.

[15] Z. Jin, Y. Xiong, K. Zhao, H. Dong, Q. Ren, H. Huang, X. Qiu, J. Xiao, P. Qiu, L. Chen, X. Shi, Abnormal thermal conduction in argyrodite-type $Ag_9FeS_{6-x}Te_x$ materials, Mater. Today Phys. 19 (2021) 100410. https://doi.org/10.1016/j.mtphys.2021.100410.

[16] J.M. Ziman, Electrons and Phonons. The Theory of Transport Phenomena in Solids, Oxford University Press, London, 1963.

[17] M. Simoncelli, N. Marzari, F. Mauri, Unified theory of thermal transport in crystals and glasses, Nat. Phys. 15 (2019) 809–813. https://doi.org/10.1038/s41567-019-0520-x.

[18] D.G. Cahill, S.K. Watson, R.O. Pohl, Lower limit to the thermal conductivity of disordered crystals, Phys. Rev. B. 46 (1992) 6131. https://doi.org/10.1103/PhysRevB.46.6131.

[19] G.A. Slack, The Thermal Conductivity of Nonmetallic Crystals, Solid State Phys. - Adv. Res. Appl. 34 (1979) 1–71. https://doi.org/10.1016/S0081-1947(08)60359-8.

[20] P.B. Allen, J.L. Feldman, J. Fabian, F. Wooten, Diffusons, locons and propagons: Character of atomic vibrations in amorphous Si, Philos. Mag. B. 79 (1999) 1715–1731. https://doi.org/10.1080/13642819908223054.

[21] M. Simoncelli, N. Marzari, F. Mauri, Wigner formulation of thermal transport in solids, 12 (2022) 041011. https://doi.org/10.1103/PhysRevX.12.041011.

[22] R. Hanus, J. George, M. Wood, A. Bonkowski, Y. Cheng, D. Abernathy, M. Manley,

G. Hautier, G.J. Snyder, R. Hermann, Uncovering design principles for amorphous-like heat conduction using two-channel lattice dynamics, Mater. Today Phys. 18 (2021) 100344. https://doi.org/10.1016/j.mtphys.2021.100344.

[23] Z. Zeng, C. Zhang, H. Yu, W. Li, Y. Pei, Y. Chen, Ultralow and glass-like lattice thermal conductivity in crystalline $BaAg_2Te_2$: Strong fourth-order anharmonicity and crucial diffusive thermal transport, Mater. Today Phys. 21 (2021) 100487. https://doi.org/10.1016/j.mtphys.2021.100487.

[24] Y. Zhou, S. Volz, Thermal transfer in amorphous superionic Li_2S, Phys. Rev. B. 103 (2021) 224204. https://doi.org/10.1103/PhysRevB.103.224204.

[25] S. Lin, W. Li, Y. Pei, Thermally insulative thermoelectric argyrodites, Mater. Today. 48 (2021) 198-213. https://doi.org/10.1016/j.mattod.2021.01.007.

[26] S. Acharya, J. Pandey, A. Soni, Enhancement of power factor for inherently poor thermal conductor Ag_8GeSe_6 by replacing Ge with Sn, ACS Appl. Energy Mater. 2 (2019) 654–660. https://doi.org/10.1021/acsaem.8b01660.

[27] T. Bernges, R. Hanus, B. Wankmiller, K. Imasato, S. Lin, M. Ghidiu, M. Gerlitz, M. Peterlechner, S. Graham, G. Hautier, Y. Pei, M.R. Hansen, G. Wilde, G.J. Snyder, J. George, M.T. Agne, W.G. Zeier, Considering the Role of Ion Transport in Diffuson-Dominated Thermal Conductivity, Adv. Energy Mater. 12 (2022) 2200717. https://doi.org/10.1002/aenm.202200717.

[28] B. Jiang, P. Qiu, H. Chen, Q. Zhang, K. Zhao, D. Ren, X. Shi, L. Chen, An argyrodite-type Ag_9GaSe_6 liquid-like material with ultralow thermal conductivity and high thermoelectric performance, Chem. Commun. 53 (2017) 11658–11661. https://doi.org/10.1039/c7cc05935c.

[29] S. Lin, W. Li, S. Li, X. Zhang, Z. Chen, Y. Xu, Y. Chen, Y. Pei, High Thermoelectric

Performance of Ag_9GaSe_6 Enabled by Low Cutoff Frequency of Acoustic Phonons, Joule. 1 (2017) 816–830. https://doi.org/10.1016/j.joule.2017.09.006.

[30] C. Yang, Y. Luo, X. Li, J. Cui, N-type thermoelectric Ag_8SnSe_6 with extremely low lattice thermal conductivity by replacing Ag with Cu, RSC Adv. 11 (2021) 3732–3739. https://doi.org/10.1039/d0ra10454j.

[31] W. Li, S. Lin, B. Ge, J. Yang, W. Zhang, Y. Pei, Low Sound Velocity Contributing to the High Thermoelectric Performance of Ag_8SnSe_6, Adv. Sci. 3 (2016) 1600196. https://doi.org/10.1002/advs.201600196.

[32] M.K. Gupta, J. Ding, D. Bansal, D.L. Abernathy, G. Ehlers, N.C. Osti, W.G. Zeier, O. Delaire, Strongly Anharmonic Phonons and Their Role in Superionic Diffusion and Ultralow Thermal Conductivity of Cu_7PSe_6, Adv. Energy Mater. 12 (2022) 2200596. https://doi.org/10.1002/aenm.202200596.

[33] Z. Zhang, Y. Guo, M. Bescond, J. Chen, M. Nomura, S. Volz, How coherence is governing diffuson heat transfer in amorphous solids, Npj Comput. Mater. 8 (2022) 1–8. https://doi.org/10.1038/s41524-022-00776-w.

[34] F. DeAngelis, M.G. Muraleedharan, J. Moon, H.R. Seyf, A.J. Minnich, A.J.H. McGaughey, A. Henry, Thermal Transport in Disordered Materials, Nanoscale Microscale Thermophys. Eng. 23 (2018) 81–116. https://doi.org/10.1080/15567265.2018.1519004.

[35] L. Isaeva, G. Barbalinardo, D. Donadio, S. Baroni, Modeling heat transport in crystals and glasses from a unified lattice-dynamical approach, Nat. Commun. 10 (2019) 3853. https://doi.org/10.1038/s41467-019-11572-4.

[36] Y. Xia, V. Ozoliņš, C. Wolverton, Microscopic Mechanisms of Glasslike Lattice Thermal Transport in Cubic $Cu_{12}Sb_4S_{13}$ Tetrahedrites, Phys. Rev. Lett. 125 (2020)

085901. https://doi.org/10.1103/PhysRevLett.125.085901.

[37] R. Hanus, R. Gurunathan, L. Lindsay, M.T. Agne, J. Shi, S. Graham, G.J. Jeffrey Snyder, Thermal transport in defective and disordered materials, Appl. Phys. Rev. 8 (2021) 031311. https://doi.org/10.1063/5.0055593.

[38] H.R. Seyf, A. Henry, A method for distinguishing between propagons, diffusions, and locons, J. Appl. Phys. 120 (2016) 025101. https://doi.org/10.1063/1.4955420.

[39] H.R. Seyf, L. Yates, T.L. Bougher, S. Graham, B.A. Cola, T. Detchprohm, M.H. Ji, J. Kim, R. Dupuis, W. Lv, A. Henry, Rethinking phonons: The issue of disorder, Npj Comput. Mater. 3 (2017). https://doi.org/10.1038/s41524-017-0052-9.

[40] R. Gurunathan, R. Hanus, M. Dylla, A. Katre, G.J. Snyder, Analytical Models of Phonon-Point-Defect Scattering, Phys. Rev. Appl. 13 (2020) 034011. https://doi.org/10.1103/PhysRevApplied.13.034011.

[41] T. Bernges, J. Peilstöcker, M. Dutta, S. Ohno, S.P. Culver, K. Biswas, W.G. Zeier, Local Structure and Influence of Sb Substitution on the Structure-Transport Properties in $AgBiSe_2$, Inorg. Chem. 58 (2019) 9236–9245. https://doi.org/10.1021/acs.inorgchem.9b00874.

[42] M.A. Kraft, S.P. Culver, M. Calderon, F. Böcher, T. Krauskopf, A. Senyshyn, C. Dietrich, A. Zevalkink, J. Janek, W.G. Zeier, Influence of Lattice Polarizability on the Ionic Conductivity in the Lithium Superionic Argyrodites Li_6PS_5X (X = Cl, Br, I), J. Am. Chem. Soc. 139 (2017) 10909–10918. https://doi.org/10.1021/jacs.7b06327.

[43] X. Shen, C.C. Yang, Y. Liu, G.G. Wang, H. Tan, Y.H. Tung, G.G. Wang, X. Lu, J. He, X. Zhou, High-Temperature Structural and Thermoelectric Study of Argyrodite Ag_8GeSe_6, ACS Appl. Mater. Interfaces. 11 (2019) 2168–2176. https://doi.org/10.1021/acsami.8b19819.

[44] N. Minafra, M.A. Kraft, T. Bernges, C. Li, R. Schlem, B.J. Morgan, W.G. Zeier, Local Charge Inhomogeneity and Lithium Distribution in the Superionic Argyrodites Li_6PS_5X (X = Cl, Br, I), Inorg. Chem. 59 (2020) 11009–11019. https://doi.org/10.1021/acs.inorgchem.0c01504.

[45] M. Tansho, H. Wada, M. Ishii, Y. Onoda, Silver ionic conductor Ag_9GaSe_6 studied by Ag and Ga NMR, Solid State Ionics 88 (1996) 155–158.

[46] J-P. Deloume, R. Faure, Un nouveau Ag_9GaSe_6 : Etude structurale de la phase alpha, J. Solid State Chem. 36 (1981) 112–117. https://doi.org/10.1016/0022-4596(81)90198-5.

[47] R.D. Shannon, Revised effective ionic radii and systematic studies of interatomic distances in halides and chalcogenides, Acta Cryst. A32 (1976) 751–767. https://doi.org/10.1107/S0567739476001551.

[48] P.B. Allen, J.L. Feldman, Thermal Conductivity of Glasses: Theory and Application to Amorphous Si, Phys. Rev. Lett. 62 (1989) 645. https://doi.org/10.1103/PhysRevLett.62.645.

[49] Z. Cheng, A. Weidenbach, T. Feng, M.B. Tellekamp, S. Howard, M.J. Wahila, B. Zivasatienraj, B. Foley, S.T. Pantelides, L.F.J. Piper, W. Doolittle, S. Graham, Diffuson-driven ultralow thermal conductivity in amorphous Nb_2O_5 thin films, Phys. Rev. Mater. 3 (2019) 025002. https://doi.org/10.1103/PhysRevMaterials.3.025002.

[50] J. Callaway, Model for Lattice Thermal Conductivity at Low Temperatures, Phys. Rev. 113 (1959) 1046. https://doi.org/10.1103/PhysRev.113.1046.

[51] G. Tan, S. Hao, R.C. Hanus, X. Zhang, S. Anand, T.P. Bailey, A.J.E. Rettie, X. Su, C. Uher, V.P. Dravid, G.J. Snyder, C. Wolverton, M.G. Kanatzidis, High Thermoelectric Performance in SnTe-$AgSbTe_2$ Alloys from Lattice Softening, Giant Phonon-Vacancy Scattering, and Valence Band Convergence, ACS Energy Lett. 3 (2018) 705–712.

https://doi.org/10.1021/acsenergylett.8b00137.

[52] M. Baggioli, B. Cui, A. Zaccone, Theory of phonon glass behaviour in host-guest thermoelectrics with avoided crossing, (2019) 1–5. http://arxiv.org/abs/1906.08079.

[53] Z. Chen, X. Zhang, S. Lin, L. Chen, Y. Pei, Rationalizing phonon dispersion for lattice thermal conductivity of solids, Natl. Sci. Rev. 5 (2018) 888–894. https://doi.org/10.1093/nsr/nwy097.

[54] G.J. Snyder, M.T. Agne, R. Gurunathan, Thermal conductivity of complex materials, Natl. Sci. Rev. 6 (2019) 380–381. https://doi.org/10.1093/nsr/nwz040.

[55] R. Gurunathan, K. Choudhary, F. Tavazza, Rapid Prediction of Phonon Structure and Properties using an Atomistic Line Graph Neural Network (ALIGNN), (2022) 1–22. http://arxiv.org/abs/2207.12510.

[56] Z. Chen, B. Ge, W. Li, S. Lin, J. Shen, Y. Chang, R. Hanus, G.J. Snyder, Y. Pei, Vacancy-induced dislocations within grains for high-performance PbSe thermoelectrics, Nat. Commun. 8 (2017) 1–8. https://doi.org/10.1038/ncomms13828.